Accepted Manuscript

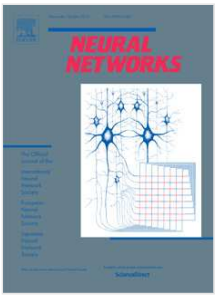

Towards biological plausibility of electronic noses: A spiking neural network based approach for tea odour classification

Sankho Turjo Sarkar, Amol P. Bhondekar, Martin Macaš, Ritesh Kumar, Rishemjit Kaur, Anupma Sharma, Ashu Gulati, Amod Kumar

PII: S0893-6080(15)00151-3
DOI: http://dx.doi.org/10.1016/j.neunet.2015.07.014
Reference: NN 3509

To appear in: *Neural Networks*

Received date: 19 September 2014
Revised date: 18 May 2015
Accepted date: 23 July 2015

Please cite this article as: Sarkar, S. T., Bhondekar, A. P., Macaš, M., Kumar, R., Kaur, R., & Sharma, A., et al. Towards biological plausibility of electronic noses: A spiking neural network based approach for tea odour classification. *Neural Networks* (2015), http://dx.doi.org/10.1016/j.neunet.2015.07.014

Towards biological plausibility of electronic noses: A spiking neural network based approach for tea odour classification

Sankho Turjo Sarkar[a,c], Amol P Bhondekar[a,c,*], Martin Macaš[d], Ritesh Kumar[a,c], Rishemjit Kaur[a,c], Anupma Sharma[a,c], Ashu Gulati[b], Amod Kumar[a,c]

[a] *CSIR-Central Scientific Instruments Organization, Chandigarh, India*
[b] *CSIR-Institute of Himalayan Bioresource Technology, HP, India*
[c] *Academy of Scientific and Innovative Research, New Delhi, India*
[d] *Czech Technical University, Prague, Czech Republic*

Abstract

The paper presents a novel encoding scheme for neuronal code generation for odour recognition using an electronic nose (EN). This scheme is based on channel encoding using multiple Gaussian receptive fields superimposed over the temporal EN responses. The encoded data is further applied to a spiking neural network (SNN) for pattern classification. Two forms of SNN, a back-propagation based SpikeProp and a dynamic evolving SNN are used to learn the encoded responses. The effects of information encoding on the performance of SNNs have been investigated. Statistical tests have been performed to determine the contribution of the SNN and the encoding scheme to overall odour discrimination. The approach has been implemented in odour classification of orthodox black tea (Kangra-Himachal Pradesh Region) thereby demonstrating a biomimetic approach for EN data analysis.

Keywords: electronic nose, McNamer's test, spiking neural network, receptive fields, spikeprop, tea, spike latency coding, dynamically evolving spiking neural networks

1. Introduction

Olfactory perception has been the essence of evolution in vertebrates and invertebrates enabling them to identify food, mates, predators and sensual pleasures as well as warnings of danger. In an olfactory system, volatile odour compounds are detected in the periphery by olfactory receptor neurons (ORNs) wherein chemical stimuli are transduced into electrical signals and are relayed

*Corresponding author
Email address: amol.bhondekar@gmail.com (Amol P Bhondekar)

to the olfactory bulb in case of vertebrates or the antennal lobe in the case of insects. The ORNs do not show any specific selectivity towards different odorants but are capable of rapidly recognising different odours as well as their intensities. Also, the anatomical and functional designs of the primary olfactory centres in insects and vertebrates are astonishingly similar suggesting the evolution of optimal odour representation schemes in biological systems [1, 2]. The advent of semiconductor and conducting polymer based gas sensor arrays and their resemblance to the mammalian olfactory system in terms of their non-selectivity led to the development of artificial olfactory systems known as electronic noses (ENs) [3].

The EN sensor response, is an analog signal whereas in biological olfactory systems binding events at olfactory receptors generate 'spikes' (discrete pulses) [4]. This dichotomy and with the increased understanding of biological olfaction mechanisms, has led to the realization of several bio-inspired artificial olfactory systems not only at the abstraction level but also at the data processing stage [4, 5]. Also, with the advent of novel bio-mimetic systems such as artificial olfactory mucosa [6–8] and an increase in the sensor array size it becomes challenging to be able to reduce the dimensionality while preserving relevant information in addition to computational overheads [7, 8]. This calls for advanced time dependent bio-inspired computational techniques to address challenging odour discrimination problems like segmentation [8].

The development of bio-inspired computational techniques for ENs has been two pronged: a bio-inspired sensor response representation, and a biologically inspired pattern recognition scheme. Various researchers have attempted to represent the gas sensor response into spikes through schemes such as rate [5] and latency coding [2, 9–11]. Spike encoding of the metal oxide semiconductor response attempted by Hsieh et al. [12], Yamani et al.[2] and Chen et al. [11] use the percentage resistance change and the logarithm of peak resistance which do not take into account the temporal information of the sensor response which in fact is the essence of EN data. These steady state methods take into account only stationary information of the sensor response and all the information related to the adsorption/desorption kinetics of the sensors and molecular dispersion of the analytes is lost [13]. Moreover, recent evidences supported by electrophysiological recordings in the olfactory bulb of awake mice prove that the temporal encodings relative to the respiratory cycle are responsible for odour perception [14]. This inspires for the development of a temporal spike encoding scheme for transforming the temporal EN sensor response. Traditionally, two hypotheses for olfactory encoding are accepted, namely, *labelled-line* and *across-fibre pattern*. The *labelled-line* theory suggests that each receptor has a narrow molecular receptive range whereas the *across-fibre pattern* theory suggests a broad molecular receptive range. The *across-fibre pattern* coding is analogous to the channel/population coding strategy, wherein, a stimulus dimension is encoded by the relative activity of a limited number of receptors with smooth and overlapping sensitivity profiles or receptive fields (RFs) [15, 16]. The advantages of channel coding in terms of less number of encoded features, no metamery, and versatility makes it optimal in many situations, as becomes especially clear in

their abundant presence in perceptual systems of biological origin [15]. Taking inspiration from this channel coding scheme, we encode the temporal response of the EN using RFs having Gaussian sensitivity profiles distributed temporally over the sniff cycle of the EN. Recent efforts towards mimicking biological neuron type computation and information transfer has led to the development of neural networks such as the spiking neural network (SNNs) [17, 18]. Researchers have used these SNNs to successfully develop bio-mimicking pattern recognition schemes for the ENs [6, 9, 19–29]. Along these lines, we use the SNN for odour discrimination over the temporal spike codes.

In this paper, we develop an encoding scheme which emulates the across-fiber or channel encoding properties of biological systems to encode the temporal dynamics of the EN sensor response. In contrast to the previously described methods of sensor response encoding which encodes only the steady state response [2, 11, 12], we have been able to capture a wide range of sensor response through RFs distributed temporally over the entire sniff cycle. Additionally, methods which tend to capture the temporal response in spikes use rate-codes thereby generating dense spike patterns [4, 5]. The spike encoding scheme introduced in this work, uses multiple Gaussian RFs which generate smaller spike codes and resulting in odour discrimination as is evident from the classification results described in the results and discussion section. The spike pattern, generated by the superposition of the RFs with the EN sensor responses is fed to a SNN for odour discrimination. This approach has been tested on the Kangra orthodox black tea odour dataset generated by the Alpha M.O.S FOX 3000 EN system. Two different learning methods using SNN were applied: an error-backpropagation method, widely used in spike-rate based neural networks, i.e., artificial neural networks (ANN), and a method based on synaptic plasticity, the dynamically evolving spiking neural network (DeSNN) [30]. Further, performance of an ANN was compared with that of a SNN using the error-backpropagation learning method [31]. Also, learning performance was compared when using ANN over the RF generated spike train and with the temporal sensor responses. The results demonstrate the effectiveness of the spike encoding method and applicability of the SNN based pattern recognition scheme. Further, due to the simplicity of the spike-encoding approach and implementation of SNN in very-large-scale-integration (VLSI) chips [20] the proposed approach can be easily ported to hardware.

2. Methodology

2.1. Sample Collection, Preparation and Data Acquisition

Four grades of Kangra orthodox black tea obtained from the "The Palampur Co-operative Tea Factory Limited", Palampur, Himachal Pradesh, India have been taken for our study. The grading of samples was done by the quality assurance team of the factory according to the internationally accepted black tea grading methodology based upon particle size and appearance [32, 33] namely SFTFOP-1 (Super Fine Tippy Flowery Orange Pekoe), TGBOP (Tippy Golden

Table 1: EN operating parameters

Parameters	Value
Incubation Time	120s
Incubation Temparature	55° C
Agitation Speed	500rpm
Agitation Time	10s
Syrienge Temparature	60° C
Injection Speed	250µl/s
Injection Volume	500µl
Sensor Chamber Temparature	65° C
Acquisition Time	100s
Acquisition Delay	800s
Acquisition Period	1s

Broken Orange Pekoe), GOF (Golden Orange Fannings) and FOF (Flowery Orange Fannings). Thus, 12 tea samples belonging to 4 classes were obtained (3 samples per class).

An EN system 'Alpha M.O.S FOX 3000', comprising of 12 Metal Oxide Semiconductor gas sensors, has been used for data acquisition. 0.5g of ground sample was soaked in 1ml of distilled water in 10ml standard vials and the Autosampler and EN parameters were optimized and set as per Table 1. 16 sniffs each of 12 tea samples belonging to 4 different classes were obtained to get 192 EN responses (each EN response consists of 12 sensors) for 100s duration with 1s sampling interval. Although, the responses of all the 12 sensors were recorded, only 4 sensors were used for classification purpose to reduce the input data size. These sensors were chosen as they mapped the maximum variability amongst the complete dataset primarily due to their specificity/non-specificity towards Terpenoids and Non-Terpenoids present in the tea samples. The sensors chosen were LY2/G, LY2/gCT, LY2/GH and LY2/gCT1 (as designated by Alpha M.O.S).

2.2. The Olfactory Receptor Unit

The sniffing cycle of an EN has 3 phases as shown in Fig. 2. In the reference phase, a carrier gas is flushed over the sensor array to obtain the baseline values, in the sniffing phase, the sensor is exposed to the odour sample causing change in the sensor response and in the last phase, called as the recovery phase, the odour sample is flushed out of the sensing chambers. This temporal data needs to be encoded into spikes using biologically inspired techniques as previously discussed, which can further be fed into an SNN for pattern recognition. Channel encoding with multiple temporal Gaussian RFs overlapped over the EN sensor data has been implemented in this work and is referred to as the Olfactory Receptor Unit (ORU). Fig. 1 represents the ORU and the spike

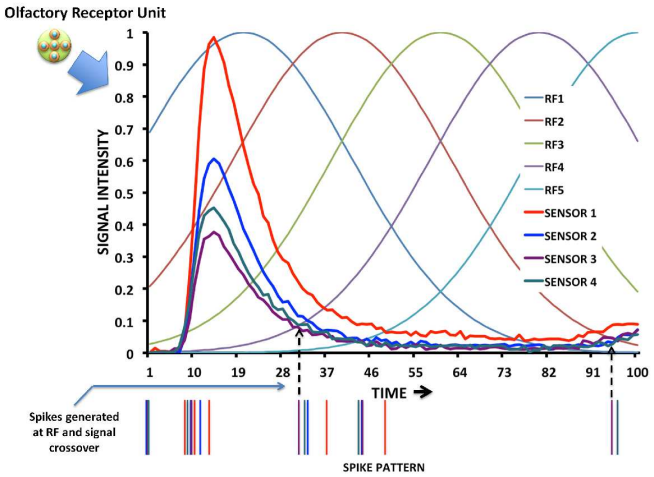

Figure 1: Encoding a sample sensor response into a spike pattern.

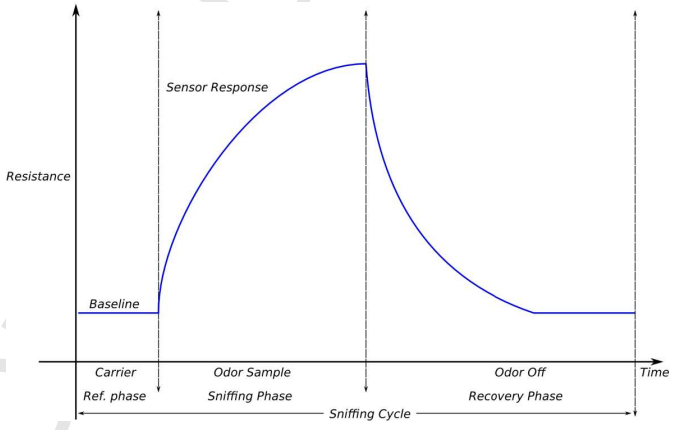

Figure 2: A typical time varying sensor response

coding scheme. It may be noted that for each sensor there is a dedicated ORU, and all the sensor responses have been superimposed as depicted in Fig. 1. The operation of the ORU can be mathematically formulated as follows:

The time series response of the i^{th} sensor ($\overrightarrow{S_i}$) is normalized ($\hat{S}_i$) based on the range of each sensor according to Eq. 1.

$$\hat{S}_i = \frac{\overrightarrow{S_i} - min(\overrightarrow{S_i})}{max(\overrightarrow{S_i}) - min(\overrightarrow{S_i})} \tag{1}$$

The spike pattern is generated by the crossover of sensor response to each of the Gaussian RFs as shown in Eq. 2. The RFs are defined as Gaussian functions (scaled to [0,1]) with $\sigma = (t_{max} - t_{min})/\gamma(m-2)$ where γ= 1.5, m is the number of RFs and $t_{max} - t_{min}$ is the time range of the sensor response [31, 34]. The points of crossover of the response with the k^{th} RF ($rf^{(k)}(t)$) is then :

$$\overrightarrow{I}_i^{(k)} = \{t : rf^{(k)}(t) = \hat{S}_i(t), 0 \leq t \leq T_{simulation}\} \tag{2}$$

It has been suggested in [10] that largest meaningful information in an olfactory system is transmitted at the first spike of the neurons. This motivates us to present the first time of intersection of the sensor response with the RFs to the network as the spike times $\overrightarrow{T}$ as is given in Eq. 3 :

$$\overrightarrow{T} = \{I_i^{(k)}(0) : 1 \leq i \leq n_{sensors}, 1 \leq k \leq n_{RF_s}\} \tag{3}$$

The spike pattern hence produced (as shown in Fig. 1) is scaled into a 10ms window [24] and presented to the SNN to reduce its simulation time without losing any information.

2.3. Network Architecture

SNNs are a special class of ANNs, wherein information amongst the neurons propagate in terms of temporally coded sequences of spikes. SNNs are generally considered to be much more biologically realistic than other neural networks [17, 18] and are particularly suitable for solving temporal pattern recognition problems [35]. Also, it has been argued that SNN implementation by analog VLSI rather than digital VLSI may reduce the power and silicon area of the chip [20] thereby envisaging a truly bio-mimetic ENs. Although SNNs have a similar architecture as in conventional neural networks they differ in the number of synaptic terminals between each layer of neurons and their corresponding synaptic delays. The behaviour of the spiking neurons has been studied and several mathematical models have been proposed namely, Hodgkin-Huxley [31], Leaky-Integrate and Fire [36], Izhikevich [37] and Spike Response(SRM) [38, 39]. In this work a 3 layered fully connected feedforward SNN with multiple delayed synaptic terminals has been implemented as shown in Fig. 3 and SRM has been adopted as the neuronal model. The output of the EN sensors (Fig. 1) is fed to an ORU, which generates a spiking pattern based upon the first crossover time of the sensor response with each RF. The spiking pattern from the ORUs are

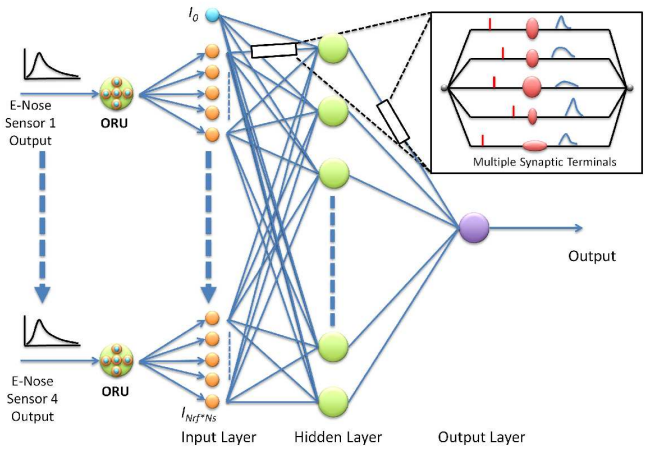

Figure 3: Structure of the fully connected feed-forward SNN network with delayed synaptic connections

then fed to the neurons in the input layer consisting of $N_{rf}xN_S$ (i.e. number of RFs x number of sensors). An additional bias neuron (I_0) having a reference spike at T_0 is added [31]. The output layer consists of a single neuron whose spike time T_{out} indicates the class of the sample. Intermediate to these two layers is the hidden layer having variable yet predetermined number of neurons $H_{1..m}$.

The gradient descent based SpikeProp algorithm requires multiple delayed synapses between each neuronal connection. Hence, the input, hidden and output layers have multiple delayed synaptic connections between them as shown in Fig. 3 inset.

2.3.1. Spike Response Model

The neuron model used is an implementation of the Spike Response Model, the SRM_0 model [38]. The SRM_0 model defines the potential $u_i(t)$ of neuron i at time t as:

$$u_i(t) = \eta(t - \hat{t}_i) + \sum_j w_{ij} \sum_{t_j^{(f)}} \epsilon_0(t - t_j^{(f)}) + \int_0^\infty \kappa_0(s) I^{ext}(t - s) ds \qquad (4)$$

$$\hat{t} = t|_{u_i(t)=1} \qquad (5)$$

The neuron is assumed to have 'spiked' when its potential $u_i(t)$ exceeds the threshold of 1mV. The first part of Eq. (4) ($\eta(t - \hat{t}_i)$) defines the after-spike potential (the neuron potential after it has undergone a spike) and is approximated by a delta function (spike) followed by hyperpolarization (reset to a value

lower than its rest potential) as given in Eq. (6):

$$\eta(t) = \delta(t - \hat{t}) - \eta_0 exp\Big(-\frac{t - \hat{t}}{\tau_{recov}}\Big) \tag{6}$$

The extent of hyperpolarization is controlled by the parameter η_0 and τ_{recov} (recovery rate).

It is assumed that no excitation is provided to the neurons through current clamping, hence the external current $I^{ext}(t)$ is taken as 0. As will be discussed in the forthcoming section, the learning method (SpikeProp) and the inference scheme uses only the time of the first spike of a neuron, hence the first part of Eq. (4) ($\eta(t - \hat{t}_i)$) does not need to be evaluated. The spike response function $\epsilon_0(t)$ specifies the effect in potential of an incoming spike from a presynaptic input j to the postsynaptic neuron i and is a function of the time since its latest firing time $t_j^{(f)}$. The spike response function assumed here is:

$$\epsilon_0(t) = exp\Big(-\frac{t}{\tau_m}\Big) - exp\Big(-\frac{t}{\tau_s}\Big) \tag{7}$$

The response $\epsilon_0(t)$ is scaled according to the weight w_{ij} of the synapse between the j^{th} presynaptic neuron and i^{th} postsynaptic neuron. The values of the time constants assumed are: $\tau_m = 4.0ms$, and $\tau_s = 2.0ms$.

2.3.2. Learning using SpikeProp

The spike pattern presented to the network is learnt using SpikeProp, a supervised learning algorithm for multilayer SNNs [31]. SpikeProp is a form of the backpropagation algorithm suited for SNNs. Using gradient descent, SpikeProp modifies the weights of synaptic connections to achieve a desired spike time of an output neuron given an input pattern. SpikeProp requires each synapse of the SNN to have a number of delayed synapses for each connection between any two neurons. A pattern is presented to the network by assigning spiking times to individual neurons in the input layer. This variant of SpikeProp supports only a single spike per neuron hence number of features in the pattern directly corresponds to the size of the input layer. The weights associated with every synaptic connection is initialized with a random value in the range from 0 to 1 and further adjusted according to the following Eq. [40]:

$$\Delta w_{hi}^k = -\gamma \frac{y_h^k(t_i^a) \sum\limits_j \{\delta_j \sum\limits_k w_{ij}^k \partial y_i^k(t_j^a)/\partial t_i^a\}}{\sum\limits_{n \in \Gamma_i} \sum\limits_l w_{ni}^l \partial y_n^l(t_i^a)/\partial t_i^a} \tag{8}$$

$$y_i^k(t) = \epsilon_0(t - t_i^k) \tag{9}$$

$$\delta_i = \frac{\sum\limits_{j \in \Gamma_i} \delta_j \{\sum\limits_k w_{ij}^k \partial y_i^k(t_j^a)/t_i^a\}}{\sum\limits_{h \in \Gamma_i} \sum_l w_{hi}^l \partial y_h^l(t_i^a)/\partial t_i^a} \tag{10}$$

Where, the weight of the synaptic connection between neurons i and j having k^{th} delay is denoted by w_{ij}^k and γ denotes the learning rate; t_i^a denotes the actual spiking time of neuron i; Γ_i is the set of neurons in layer i; $\delta y_n^l(t_i^a)/\delta t_i^a$ is the change in potential of the spike response function $\epsilon_0(t)$ of neuron i and delay synapse k . The SpikeProp learning rule, when used in its original form leads to cases where neurons stop firing due to extremely low weights assigned to them. In those cases it is assumed that the neuron fires at the simulation time.

$$t_{spike}^{(i)} = \begin{cases} T_{spike}^{(i)}(0) & when \quad T_{spike}^{(i)} \neq \phi \\ T_{simulation} & when \quad T_{spike}^{(i)} = \phi \end{cases} \tag{11}$$

The output spike time is mapped directly to the predicted class by dividing the simulation time linearly according to the number of unique classes after giving an offset of 15 ms. If there are 5 unique classes and simulation time is 50 ms, then class 2 would be encoded by a spike at 29 ms. The offset of 15 ms is chosen to consider the time of entire spike pattern presentation and propagation over the neuron layers before generating the output spike. The learning error E is evaluated as:

$$E = \frac{1}{N}\sum_{n=1}^{N}(O_t(n) - O_t'(n))^2 \tag{12}$$

Where, N is the total number of patterns; $O_t(n)$ is the spiking time at the output neuron when pattern n is presented to it and $O_t'(n)$ is the desired spike time.

2.3.3. Learning with dynamically evolving spiking neural networks (deSNN)

The deSNN model, as proposed by Kasabov et al. [30], uses rank order (RO) [41] and spike time dependant plasticity (STDP) to initialise and adjust the synaptic weights respectively. In this work, such a synapse is implemented between the RFs and the output layer. The RFs are also connected to the output layer through as many inhibitory neurons as in the output layer.

Initialising the synapse weights with RO involves ordering the spikes incident on post-synaptic neurons. Based on this order, each connection weight between presynaptic neuron i and postsynaptic neuron j is initialised according to:

$$w_{j,i} = 0.8^{order_{j,i}} \tag{13}$$

where, $order_{j,i}$ is the rank of the first spike from presynaptic neuron j to the postsynaptic neuron i among all of the spikes generated at j. At the presentation of a new training pattern, an output neuron is created and its weights initialised according to the above method. Further, as spikes are incident on a neuron, the weights are drifted upwards or downwards with saturation at 0.6 and 0 respectively. The drift amount was set at 0.072 positive or negative according to whether or not the spike at the postneuron was preceded by a spike at the preneuron respectively. Output neurons with same label and equal weight vectors are merged together. During recall, when an unknown spike pattern

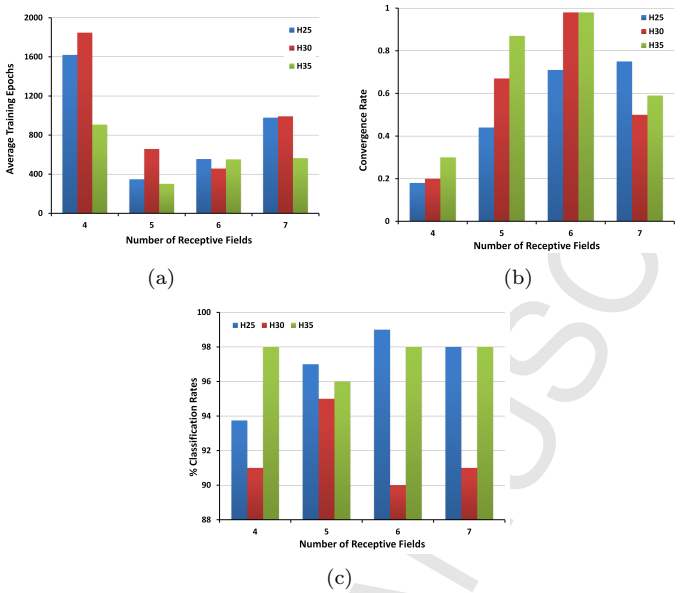

Figure 4: Variation in (a) mean epochs, (b) convergence probability, and (c) classification rate with varying RFs and HLS.

is presented, a new output neuron is created and its weights calculated. The label of the closest already learnt output neuron, with similar weight vectors is assigned to the presented pattern.

3. Results and Discussion

Experiments were performed to optimize the overall approach by individually optimizing the ORUs and SNN structure. Further, in order to determine which aspect of the model (i.e. ORU or SNN) is most important for the improvement in classification we performed two experiments. First, we compared 2 ANNs, one trained on the original sensor data and another on the spike trains. Second, we compared an ANN against an SNN, both trained on spike trains. To compare the efficiency of the learning algorithms, we further obtained the classification performance of the DeSNN algorithm, using the ORU transformed spike trains. Detailed experimentation and results have been discussed in this section.

The training and testing datasets were constructed such that sniffs obtained from each tea sample lie fully in one of the datasets. As each of the classes had only 3 tea samples, 12-fold cross-validation was used so that the 16 sniffs of any one sample from the 4 classes formed the test set and the rest formed the training set. The learning rate for the SNN and ANN was kept constant at 0.1 after empirical determination.

To optimize the overall approach, we varied the number of RFs and the

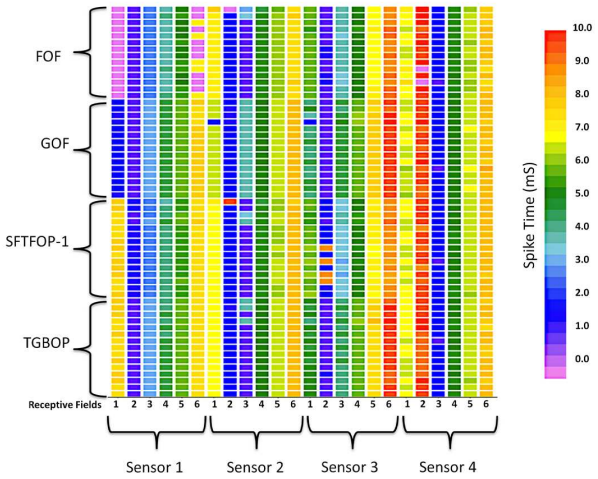

Figure 5: Neural code at the input layer for the first 15 samples of each class.

hidden layer size (HLS) and observed the training epochs required, number of classifiers which eventually converged and the final classification rate. The classifier was assumed to have converged if it attained a Mean Square Error (MSE) of 0.5. Fig. 4(a) shows the average training epochs required to attain convergence for different RF and HLS. For RF=4, the number of training epochs were observed to be exceptionally large suggesting information loss in the ORUs. Also, selecting higher values of RF (RF=7) resulted in a large number of training epochs regardless of the HLS due to increase in the total number of input neurons as the number of input neurons is proportional to the product of RFs and the number of sensors. This may also be attributed to the possibility that increasing the RFs results in redundancy of the spike code. Setting RFs to 5 resulted in minimal training epochs except for the case HLS=30. Also we observe from Fig. 4(a) that any run converges within 2000 epochs. These results were convincing to fix the maximum training epochs to 2000. Further, investigations were performed to establish the convergence guarantee by calculating the convergence probability, which is the ratio of the number of runs which converged to the total number of runs. Fig. 4(b) shows the convergence probabilities for each of the RF and HLS configurations. It can be observed that selecting 6 RFs and at least 30 HLS almost guarantees convergence.

Fig. 4(c) shows the average percentage classification rates achieved at the end of 2000^{th} epoch for each of the RF and HLS configurations (numerical values listed in Table 2). Although more than 90% classification rate was achieved for all the combinations (except for RF = 4 and HLS = 25), the maximum classification rate of 99.43% was achieved for RF = 6 and HLS = 30. Fig. 6 shows the variation in training and testing mean squared error of one of the best runs for the above mentioned configuration. Oscillations on the error surface can be

Table 2: Average classification percentage rates under various learning methods. Statistical significance (p-value) of the difference of means of the classification rates for SNN and ANN were calculated using the McNamer Test.

RFs	HLS	Classification Rate			
		SNN	ANN	p-value	DeSNN
4	25	93.75	94.27	0.500	96.67
	30	95.31	94.27	0.342	
	35	96.35	94.79	0.186	
5	25	95.31	90.62	0.013	95.33
	30	95.31	93.23	0.144	
	35	95.83	95.83	0.691	
6	25	97.92	97.40	0.500	96.67
	30	98.43	94.79	0.012	
	35	97.40	95.31	0.193	
7	25	96.35	95.83	0.500	96.67
	30	96.88	93.75	0.039	
	35	96.88	89.06	0.0001	

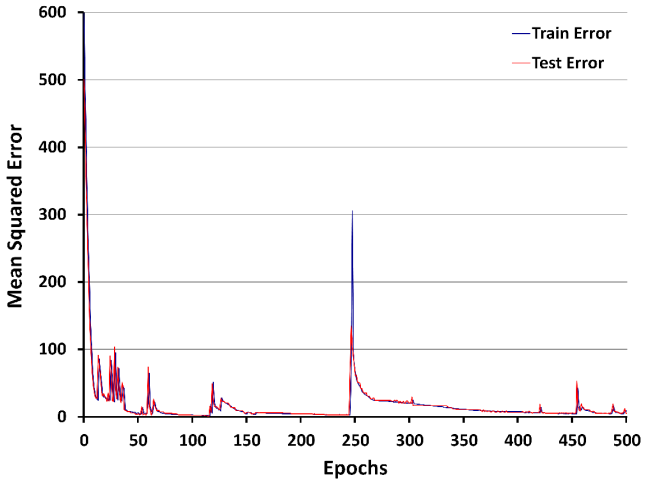

Figure 6: Variation in training and testing MSE with epochs for RF= 6 and HLS=30.

Table 3: Parameters used for the SNN and ANN

Parameter	Setting
Learning Rate	0.1
Number of hidden layers	1
HLS	25,30,35
Learning algorithm	Back-propagation gradient descent
Maximum epochs	2500
Cross-validation technique	12 fold

observed which is attributed to the fact that each neuron fires when its activity threshold is reached. The activity is the sum of spike response functions and has many local minimum due to the superpositions of spike response functions in a neuron. This causes the weights to move to local minimum while updating and eventually causing a discontinuous change of firing time and instability in the learning process, which is an inherent characteristic of SpikeProp[42, 43]. Fig. 5 shows the colour encoded spike times for the above mentioned configuration for 15 samples of each class. The temporal inter-class variability and intra-class similarity is clearly observable with respect to the RF and sensors.

To compare the contribution of the ORU and SNN to the overall classification performance, firstly, we compare the classification performance of MLP ANN over the original data and the ORU codes. Secondly, we compare the classification performance of the ANN and the SNN over the ORU codes. Table 3 lists the parameters used for the SNN and ANN classifiers. The training algorithm used for the SNN (SpikeProp) is based on the standard gradient descent, hence the same was used for training the ANN. The statistical difference in classification rates was calculated using the McNemar's test [44] according to the procedure as discussed in [45]. The McNemar's test has been used for comparison due to its low *Type 1* error and simple formulations.

Table 4 lists the classification performance along with their statistical significance using the first approach. It can be observed that the classification rate obtained using the ORUs is significantly better than while using original data for all combinations of RF and HLS. Here the significance level is considered to be $p \leq 0.05$. Also, maximum average classification rate of 94.68% was obtained with HLS and number of RFs as 30 and 6 respectively. This further strengthens the argument that this is the optimal configuration for this approach. Also, as the original time-series data is much larger (400 features) in comparison to the spike series (16-28 features, depending on number of RFs) it can be concluded that the spike-series generated from the ORUs encode the sensor response effectively.

Table 2 shows the average classification rates using various RF and HLS combinations for SNN and ANN trained with ORU spike codes and their corresponding p-values. It can be observed that in 4 out of 12 cases, SNN performed significantly better than ANN and for rest of the cases the difference in classification rates was found to be statistically insignificant. This suggests the

Table 4: Average classification rate over ORU spike-series data using multi-layer perceptron ANN with 1 hidden layer and trained using back-propagation gradient descent.

HLS	Original Data	ORU spike code		p-value
	Class. Rate	RFs	Class. Rate	
25	76.302%	4	86.562%	0.119
		5	91.927%	0.037
		6	91.042%	0.044
		7	92.448%	<0.001
30	63.594%	4	92.188%	<0.001
		5	89.948%	0.005
		6	94.688%	0.002
		7	91.823%	<0.001
35	72.344%	4	92.708%	<0.001
		5	90.312%	0.001
		6	91.146%	0.014
		7	93.802%	0.004

fact that the contribution of the ORU is more than the SNN towards overall odour discrimination. It is interesting to note that again maximum average classification rate was obtained for SNN with 6 number of RFs and 30 HLS.

Further, as can be observed from Table 2, the deSNN algorithm performs the classification task equally well for all RF sizes. However, it was able to learn the dataset in a single pass. Hence, compared to the backpropagation algorithms, the deSNN algorithm is much more efficient than SpikeProp.

4. Conclusion

An SNN with a novel technique of encoding the temporal data into spikes was implemented for investigating its applicability towards odour recognition. The proposed method successfully classified the Kangra orthodox black tea odour data presented to it. The work has shown that channel encoding with multiple Gaussian RFs overlapped over the EN sensor data can be used as a neuronal encoding scheme in order to classify the EN data. Network architecture and ORUs were optimised for the aforementioned purpose by studying the influence of the number of RFs and SNN size. Results indicate significantly better classification performance with ORU codes rather than with the original data. However, the SNN produced better classification than the ANN in only a few combinations of number of RFs and hidden layer sizes. The deSNN algorithm, operating in combination with the ORUs, also performed comparably for the classification task. Thus, such combination of receptive field based population coding with deSNN models can further be explored to perform real time learning of temporal sensor responses.

Encoding each ORU independently by determining the optimal number of RFs, their position and spread is a matter of further investigation. The limitations of the learning algorithm (SpikeProp) necessitate a bigger architecture and thus is computationally slower. Therefore as a future work, integration of ORUs with other faster SNN learning algorithms based on gradient descent such as QuickProp and RProp and algorithms which handle multiple spikes per neuron such as MuSNN is envisaged. The efficacy of the encoding scheme on standard odorants with varying concentration demands further investigation.

Acknowledgement

The authors are thankful to the management of "The Palampur Co-Operative Tea Factory Ltd.", Palampur, Himachal Pradesh, India for providing tea samples, Dr Ashu Gulati, Scientist, CSIR-IHBT, Palampur for her valuable guidance and Monika Singla and Anupama Sharma for sample collection.

References

[1] B. W. Ache, J. M. Young, Olfaction: diverse species, conserved principles., Neuron 48 (3) (2005) 417–430. doi:10.1016/j.neuron.2005.10.022.

[2] J. Al Yamani, F. Boussaid, A. Bermak, D. Martinez, Glomerular latency coding in artificial olfaction, Frontiers in neuroengineering 4 (18). doi:10.3389/fneng.2011.00018.

[3] K. Persaud, G. Dodd, Analysis of discrimination mechanisms in the mammalian olfactory system using a model nose., Nature 299 (5881) (1982) 352–355.

[4] E. Martinelli, A. D Amico, C. Di Natale, Spike encoding of artificial olfactory sensor signals, Sensors and Actuators B: Chemical 119 (1) (2006) 234–238.

[5] T. C. Pearce, P. F. M. J. Verschure, J. White, J. S. Kauer, Stimulus encoding during the early stages of olfactory processing: A modeling study using an artificial olfactory system, Neurocomputing 38 (2001) 299–306.

[6] J. A. Covington, J. W. Gardner, A. Hamilton, T. C. Pearce, S.-L. Tan, Towards a truly biomimetic olfactory microsystem: an artificial olfactory mucosa, Nanobiotechnology, IET 1 (2) (2007) 15–21.

[7] J. W. Gardner, J. E. Taylor, Novel convolution-based signal processing techniques for an artificial olfactory mucosa, Sensors Journal, IEEE 9 (8) (2009) 929–935. doi:10.1109/JSEN.2009.2024856.

[8] J. W. Gardner, S.-L. Tan, J. A. Covington, T. C. Pearce, Enhanced Discrimination of Complex Odours Based upon Spatio-Temporal signals from a Micro-Mucosa, in: Solid-State Sensors, Actuators and Microsystems Conference, 2007. TRANSDUCERS 2007. International, IEEE, 2007, pp. 2465–2468.

[9] J. White, J. S. Kauer, Odor recognition in an artificial nose by spatio-temporal processing using an olfactory neuronal network, Neurocomputing 26 (1999) 919–924.

[10] E. Martinelli, D. Polese, F. Dini, R. Paolesse, D. Filippini, I. Lundström, C. Di Natale, An investigation on the role of spike latency in an artificial olfactory system, Frontiers in neuroengineering 4.

[11] H. T. Chen, K. T. Ng, A. Bermak, M. K. Law, D. Martinez, Spike latency coding in biologically inspired microelectronic nose, Biomedical Circuits and Systems, IEEE Transactions on 5 (2) (2011) 160–168.

[12] H.-Y. Hsieh, K.-T. Tang, Hardware Friendly Probabilistic Spiking Neural Network With Long-Term and Short-Term Plasticity, IEEE Transactions on Neural Networks and Learning Systems 24 (12) (2013) 2063–2074. doi:10.1109/TNNLS.2013.2271644.

[13] R. Kaur, R. Kumar, A. Gulati, C. Ghanshyam, P. Kapur, A. P. Bhondekar, Enhancing electronic nose performance: A novel feature selection approach using dynamic social impact theory and moving window time slicing for classification of Kangra orthodox black tea (Camellia sinensis (L.) O. Kuntze), Sensors and Actuators B: Chemical.

[14] M. Smear, R. Shusterman, R. O. Connor, T. Bozza, D. Rinberg, Perception of sniff phase in mouse olfaction, Nature 479 (7373) (2011) 397–400.

[15] H. Snippe, J. Koenderink, Discrimination thresholds for channel-coded systems, Biological Cybernetics 66 (6) (1992) 543–551. doi:10.1007/BF00204120.
URL http://dx.doi.org/10.1007/BF00204120

[16] S. J. Thorpe, A. Delorme, R. VanRullen, Spike-based strategies for rapid processing, Neural networks 14 (6-7).

[17] W. Maass, Networks of spiking neurons: the third generation of neural network models, Neural networks 10 (9) (1997) 1659–1671.

[18] A. K. NSKI, F. Ponulak, Introduction to Spiking Neural Networks: Information processing, learning and applications, ACTA Neurobiol Exp 71 (2011) 409–433.

[19] H.-Y. Hsieh, K.-T. Tang, A spiking neural network chip for odor data classification, in: Circuits and Systems (APCCAS), 2012 IEEE Asia Pacific Conference on, 2012, pp. 88–91. doi:10.1109/APCCAS.2012.6418978.

[20] H.-Y. Hsieh, K.-T. Tang, VLSI Implementation of a Bio-Inspired Olfactory Spiking Neural Network, Neural Networks and Learning Systems, IEEE Transactions on 23 (7) (2012) 1065–1073. doi:10.1109/TNNLS.2012.2195329.

[21] H. S. Abdel-Aty-Zohdy, J. N. Allen, Sampling Spiking Neural Network electronic nose on a tiny-chip, in: Circuits and Systems (MWSCAS), 2010 53rd IEEE International Midwest Symposium on, 2010, pp. 81–84. doi:10.1109/MWSCAS.2010.5548566.

[22] J. N. Allen, S. B. Hasan, H. S. Abdel-Aty-Zohdy, R. L. Ewing, An E-nose haar wavelet preprocessing circuit for spiking neural network classification, in: Circuits and Systems, 2008. ISCAS 2008. IEEE International Symposium on, 2008, pp. 2178–2181. doi:10.1109/ISCAS.2008.4541883.

[23] A. Gutierrez-Galvez, R. Gutierrez-Osuna, Increasing the separability of chemosensor array patterns with Hebbian/anti-Hebbian learning, Sensors and Actuators B: Chemical 116 (1) (2006) 29–35.

[24] J. White, T. A. Dickinson, D. R. Walt, J. S. Kauer, An olfactory neuronal network for vapor recognition in an artificial nose, Biological cybernetics 78 (4) (1998) 245–251.

[25] B. Raman, R. Gutierrez-Osuna, Chemosensory processing in a spiking model of the olfactory bulb: chemotopic convergence and center surround inhibition, feedback 2 (2004) 3.

[26] B. Raman, T. Kotseroglou, L. Clark, M. Lebl, R. Gutierrez-Osuna, Neuromorphic processing for optical microbead arrays: dimensionality reduction and contrast enhancement, Sensors Journal, IEEE 7 (4) (2007) 506–514.

[27] L. Ratton, T. Kunt, T. McAvoy, T. Fuja, R. Cavicchi, S. Semancik, A comparative study of signal processing techniques for clustering microsensor data (a first step towards an artificial nose), Sensors and Actuators B: Chemical 41 (1) (1997) 105–120.

[28] J. Ambros-Ingerson, R. Granger, G. Lynch, Simulation of paleocortex performs hierarchical clustering., Science.

[29] B. Raman, J. L. Hertz, K. D. Benkstein, S. Semancik, Bioinspired methodology for artificial olfaction, Analytical chemistry 80 (22) (2008) 8364–8371.

[30] N. Kasabov, K. Dhoble, N. Nuntalid, G. Indiveri, Dynamic evolving spiking neural networks for on-line spatio- and spectro-temporal pattern recognition, Neural Networks 41 (2013) 188–201.

[31] S. M. Bohte, J. N. Kok, H. La Poutre, Error-backpropagation in temporally encoded networks of spiking neurons, Neurocomputing 48 (1) (2002) 17–37.

[32] S. Borah, E. L. Hines, M. Bhuyan, Wavelet transform based image texture analysis for size estimation applied to the sorting of tea granules, Journal of Food Engineering 79 (2) (2007) 629–639.

[33] Grading, sorting and packing, \url{http://www.tocklai.net/TeaManufacture/sorting.aspx} (Oct. 2011).
URL `http://www.tocklai.net/TeaManufacture/sorting.aspx`

[34] A. Hojjat, S. Ghosh-Dastidar, Automated EEG-based Diagnosis of Neurological Disorders: Inventing the Future of Neurology, CRC Press, 2010.

[35] S. Ghosh-Dastidar, H. Adeli, Spiking Neural Networks, International Journal of Neural Systems 19 (04) (2009) 295–308. doi:10.1142/S0129065709002002.
URL `http://www.worldscientific.com/doi/abs/10.1142/S0129065709002002`

[36] T. Natschläger, B. Ruf, Spatial and temporal pattern analysis via spiking neurons, Network: Computation in Neural Systems 9 (3) (1998) 319–332.

[37] E. M. Izhikevich, Simple model of spiking neurons, Neural Networks, IEEE Transactions on 14 (6) (2003) 1569–1572.

[38] W. M. K. Wulfram Gerstner, Spiking Neuron Models: Single Neurons, Populations, Plasticity, Cambridge University Press, 2002.

[39] W. Maass, C. M. Bishop, Pulsed neural networks, The MIT Press, 2001.

[40] Q. X. Wu, T. M. McGinnity, L. P. Maguire, B. Glackin, A. Belatreche, Learning under weight constraints in networks of temporal encoding spiking neurons, Neurocomputing 69 (16) (2006) 1912–1922.

[41] S. Thorpe, J. Gautrais, Rank order coding, in: Computational Neuroscience, Springer, 1998, pp. 113–118.

[42] W. Toshiki, T. Haruhiko, K. Hiroharu, T. Shinji, A training algorithm for SpikeProp improving stability of learning process, in: Neural Networks (IJCNN), The 2011 International Joint Conference on, IEEE, 2011, pp. 951–955.

[43] F. Masaru, T. Haruhiko, K. Hidehiko, H. Terumine, Shape of error surfaces in SpikeProp, in: Neural Networks, 2008. IJCNN 2008. (IEEE World Congress on Computational Intelligence). IEEE International Joint Conference on, 2008, pp. 840–844.

[44] B. Bostanci, E. Bostanci, An Evaluation of Classification Algorithms Using Mc Nemar's Test, Proceedings of Seventh International Conference on Bio-Inspired Computing: Theories and Applications (BIC-TA 2012) 201. doi:10.1007/978-81-322-1038-2.
URL `http://link.springer.com/10.1007/978-81-322-1038-2`

[45] S. J. H. U. Salzberg, On Comparing Classifiers : Pitfalls to Avoid and a Recommended Approach, Data Mining and knowledge discovery 328 (1997) 317–328.

List of Figures